3D-CFD NUMERICAL MODELING OF IMPACTS FROM HORIZONTAL AXIS TIDAL TURBINES IN THE NEAR REGION

Sufian Fuad Sufian[1] and Ming Li[1]

A Virtual Blade Model approach has been applied to simulate flows across a Horizontal Axis Tidal Turbine (HATT). The 3D-CFD Fluent 14.5 package was employed to solve the Reynolds Averaging Navier Stokes equations. A source term was added in the momentum equation as part of the solution developed through the Blade Element Momentum Theory for an incompressible flow in a open channel. The model was validated against experimental data of a 3 bladed 0.5m diameter turbine in a high speed re-circulating water flume in terms of velocity and Turbulent Kinetic Energy (TKE) profiles. The model results correlate well with the experimental data. The change of flow field and the variation of free surface can be clearly seen in the results.

Keywords: wake characteristics; virtual blade model; horizontal axis tidal turbine; open channel; Numerical model; university of Liverpool

INTRODUCTION

Concerns regarding climate change and the danger of natural resources depleting, it has become increasingly necessary for international communities to fully exploit the natural renewable energy resources. Tidal power has been identified as a fairly good energy sources due to the fact that it is highly predictable and reliable. Horizontal Axis Tidal Turbine (HATT) is currently the most popular type of tidal energy device that bears many similarities with the wind turbines (Douglas et al. 2008). However, so far the fundamental understandings of HATT impacts on the marine environment are still far from satisfactory. In particular, most of the previous studies are limited to idealised one dimensional steady flow. The representation of a tidal turbine operation also has been much simplified as a static uniform porous disk. To enable the realistic engineering design, it has become critical to better understand the impact of turbine operations on the hydrodynamics in the complex natural conditions. A modified geometry of a traditional uniform porous disk was adopted to accommodate a numerical Virtual Blade Model (VBM) approaches for simulating a HATT. The current study focuses on extending the existing models capability to include variations of free surface as well as unsteady flows. The model is validated against laboratory measurements for a 3 bladed 0.5m diameter HATT in a high speed flume (Tedds et al. 2012). Mozafari (2010) compared three different numerical methods and suggested that VBM is an ideal compromise. Written by Barnsley and Wellicome (1993), VBM was first used in the aerodynamic sector particularly in helicopter rotor designs (Michael 2005). During recent years VBM has become popular and found its way into the tidal sector. Williams et al (2010) used VBM to simulate a HATT using real site data. He concluded that wake recovery is greatly influenced by the nature of stream floor. Malki et al (2013) coupled VBM with CFD to explain wake characteristics at different HATT emersions. He validated the model results against experimental data of power coefficient. The common fact in both studies is the absence of a free surface. Consul et al (2011), however, has demonstrated that the free surface effects can be important as the errors tend to occur if a rigid lid approach is employed. In this study the model is validated against experimental data in terms of velocities and Turbulence Kinetic Energy. All aspects of turbulence are accounted for besides roughness along the channel bed. The impact of HATT on the free surface was also assessed.

NUMERICAL METHOD

The 3D CFD package FLUENT 14.5 was employed to resolve the details of flow around and behind a HATT. The Reynolds Average Nervier-Stokes equations were solved using the finite volume method (ANSYS 2010), see Eq. 1 & 2. The Reynolds stress term $\left(-\rho\overline{u'_\iota u'_\jmath}\right)$ in Eq. 1 is resolved through different turbulence models. In the present study, a two equation turbulence model, Shear Stress Transport k-ω, is adopted to simulate turbulence generation and dissipation. It uses the k- ω formulation for both inner parts and at the wall through the viscous sub layer and switches to k-e in the free stream which unites the advantages of both methods (Menter 1993).

$$\frac{\partial}{\partial t}(\rho u_i) + \frac{\partial}{\partial x_i}(\rho u_i u_j) = -\frac{\partial p}{\partial x_i} + \frac{\partial}{\partial x_j}\left[\mu\left(\frac{\partial u_i}{\partial x_j} + \frac{\partial u_j}{\partial x_i} - \frac{2}{3}\delta_{ij}\frac{\partial u_l}{\partial x_l}\right)\right] + \frac{\partial}{\partial x_j}\left(-\rho\overline{u'_i u'_j}\right) \quad (1)$$

$$\frac{\partial \rho}{\partial t} + \frac{\partial}{\partial x_i}(\rho u_i) = 0 \quad (2)$$

where μ is the molecular viscosity, ρ is density, p is pressure, $\bar{u}_i$ and u'_i are the mean and fluctuating velocities respectively. The Volume of Fluid (VOF) model is adapted to simulate the free surface variations. It is a

[1] Centre for Engineering Sustainability, University of Liverpool, Brownlow Hill, Liverpool, L69 3GQ, United Kingdom.

surface-tracking technique applied to a fixed Eulerian mesh. A single set of momentum equations is shared by the fluids and the volume fraction of each of the fluids in each computational cell is tracked throughout the domain. Eq. 3 presents the water phase equation that performs by taking the solution of the continuity equation for the phase.

$$\frac{1}{\rho_w}\left[\frac{\partial}{\partial t}(\alpha_w\rho_w) + \nabla.(\alpha_w\rho_w\vec{v}_w) = \sum_{A=1}^{n}(\dot{m}_{Aw} - \dot{m}_{wA})\right] \quad (3)$$

where $\dot{m}_{Aw}$ and $\dot{m}_{wA}$ is the mass transfer from air to water and vice versa respectively. α_w, ρ_w *and* $\vec{v}_w$ are the water fraction, density and velocity. The tidal turbine operation is represented via VBM, which simulates the effect of the rotating blades on the fluid through a body force in the x, y and z direction. It acts inside the disk volume using a source term in the momentum equation, Eq. 4. The source term develops as a part of the solution by the use of Blade Element Theory.

$$\frac{\partial}{\partial t}(\rho u_i) - \frac{\partial}{\partial x_i}(\rho u_i u_j) = -\frac{\partial p}{\partial x_i} + \frac{\partial}{\partial x_j}\left[\mu\left(\frac{\partial u_i}{\partial x_j} + \frac{\partial u_j}{\partial x_i} - \frac{2}{3}\delta_{ij}\frac{\partial u_k}{\partial x_k}\right)\right] + \frac{\partial}{\partial x_j(-\rho\overline{u'_i u'_j})} + \overrightarrow{S_{cell}} \quad (4)$$

Bernoulli's equation is applied assuming the flow is frictionless; therefore the axial(a), angular(a') induction factors and λ_r the tip speed ratio can defined the effective angle of attack β on blades.

$$\tan\beta = \frac{\lambda_r(1+a')}{(1-a)} \quad (5)$$

The blade is divided into sections at a fixed radius. The effect of drag and torque (Tangential) forces are calculated on each section of the blade as follows:

$$S_x = dF_x = B0.5\rho w^2(C_L\sin\beta + C_D\cos\beta)cdr \quad (6)$$

$$S_\theta = dF_{\theta=}dT = B0.5\rho w^2(C_L\cos\beta + C_D\sin\beta)crdr \quad (7)$$

$$B = \frac{2\sigma'\pi r}{c} \quad (8)$$

where B is the number of blades, σ' is the local solidity and c is the chord length. Values of C_L and C_D are obtained from lookup tables which are established either experimentally or theoretically using XFOIL (Drela 2001). S_x and S_θ are the source terms in axial and tangential directions respectively. These source terms are substituted in Eq. 4 in the form S_i.

MODEL SETUP

The model is setup for a laboratory test which was carried out in a High Speed Flume. The flume has dimensions of 7m long, 1.4m wide and 1.4m deep. The HATT has a diameter of 0.5m, located at centre point of channel, mid depth of water section and 1.75m away from inlet. Fig. 1 below represents the model dimensions.

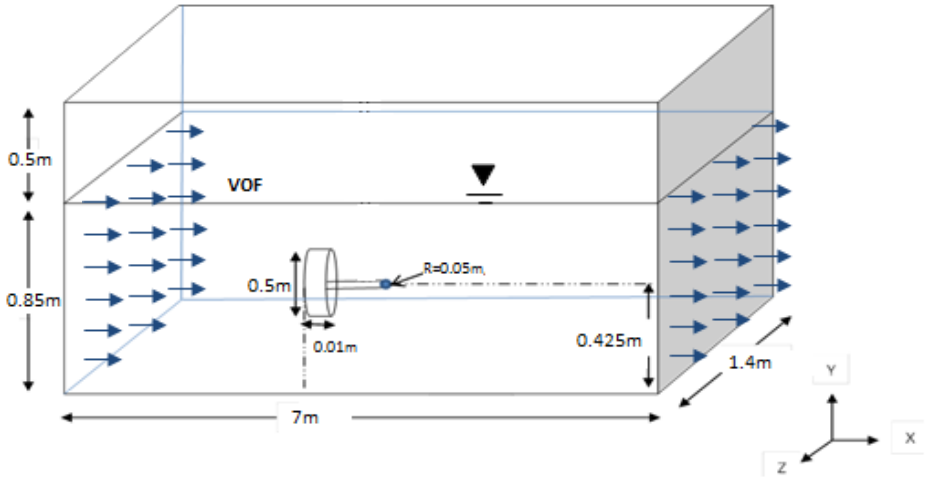

Fig 1. Model description.

The turbine consists of 3 blades rotating at TSR = 5.5. The blade collective pitch is 6 degrees. The channel inlet velocity is 0.9 m/s with a turbulence intensity of 3%. Measurements of flow velocity in the x, y and z directions and Turbulent Kinetic Energy were taken at 5 locations with an interval of 0.5m (1 diameter) downstream, see Fig. 2 and 3.

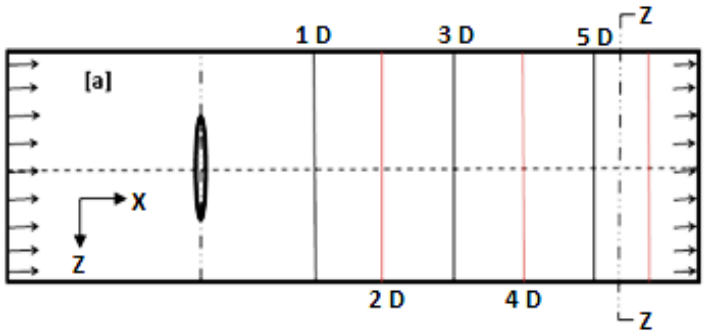

Fig 2. Plan view: represents measurement lines.

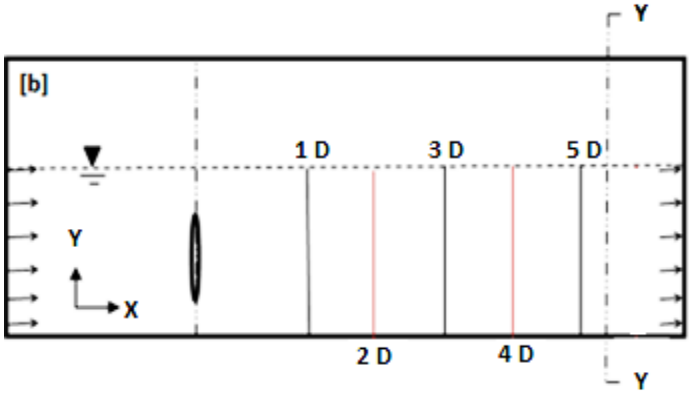

Fig 3. Side view: represents measurement lines.

DISSCUSION

The model results were found to be highly time-dependent due to the operation of the turbine and the eddy shedding behind the device. To compare with the measurements, the results were collected at intervals of 0.07s for a period of 4s and then averaged to obtain the mean flows. In Fig. 4, it can be seen clearly that the computed horizontal velocity in x-direction clearly shows a "W" distribution at 1.0m downstream of the turbine, which is due to the rotation of the turbine and the interactions with the surrounding flows. In previous studies where porous mediums were employed, CFD result does not show such a velocity profile distribution, simply because the disks approach is not able to produce the same near field effects to the surrounding flows as the turbine rotation. With the VBM implemented, the flow velocity profiles are better approximated. At the 3m downstream, it is clear that the effects of the turbine rotation has been minimised and the reduced flow profile is fairly close to that behind a static obstacle in the water. In both site, the computed results correlate closely with the experimental data.

When the flow strikes the HATT, the hub reduces flow velocity and forces the flow to diffract around it through the blade to hub connector pin gap allowing higher velocity through. This causes revered flows directly behind the hub. Moving further up the blade span, the flow velocity continues to reduces reaching minimum at blade tip. Subsequently the flow velocity begins to increase reaching a maximum speed of 1.1m/s at +/-0.35m away from hub, see Fig. 5.

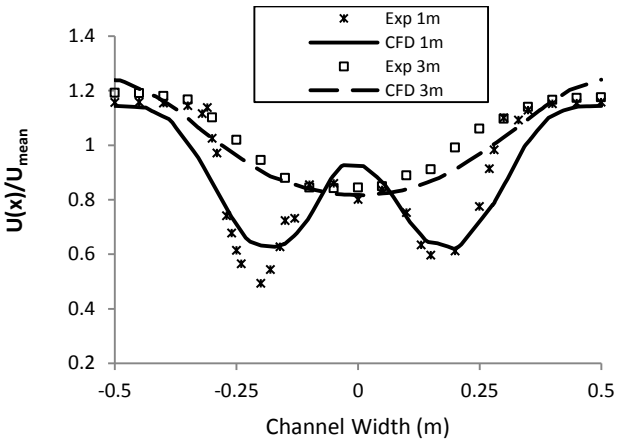

Fig 4. Comparison between experimental data and computed horizontal velocity results across the channel at 1 and 3m downstream.

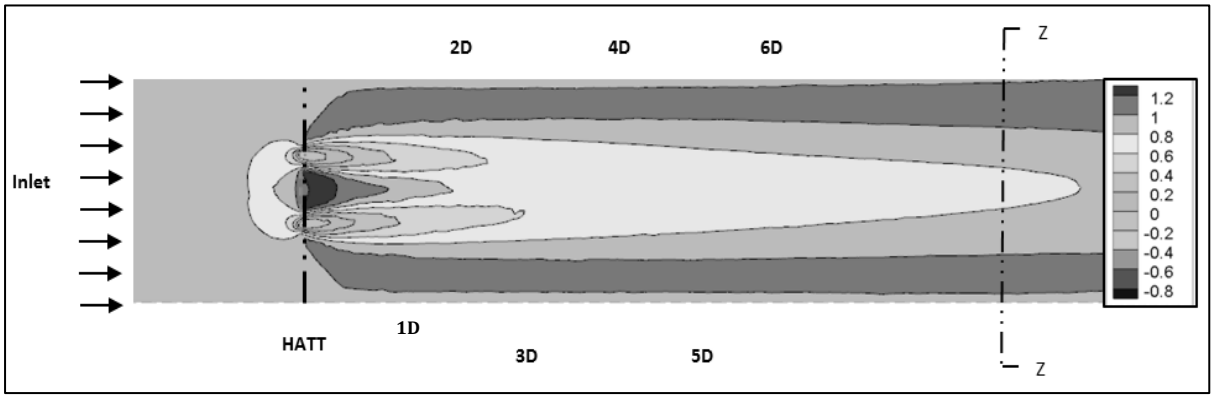

Fig 5. Plan view: represents the velocity contour map.

The rotational motion of the HATT is demonstrated in Fig. 6 which illustrates the vertical velocity in y direction indicating a clockwise rotation. Although the HATT blades are not explicitly resolved in the model, the upwards and downward flow around the turbine blade tip are still clearly seen in the figure. Fig. 7 illustrates the lateral velocity in z direction, indicating that the wake is moving inwards towards the centre line. Comparing with the results in Fig 4, it is clear that the flow is dominant in the horizontal direction with the largest velocity magnitude.

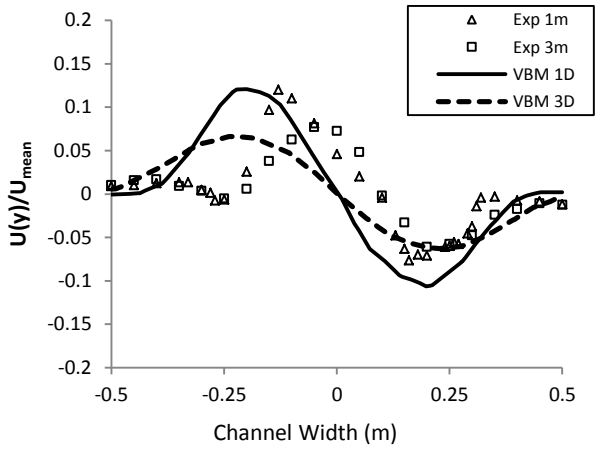

Fig 6. Comparison between experimental and computed vertical velocities across the channel at 1 and 3 meters downstream.

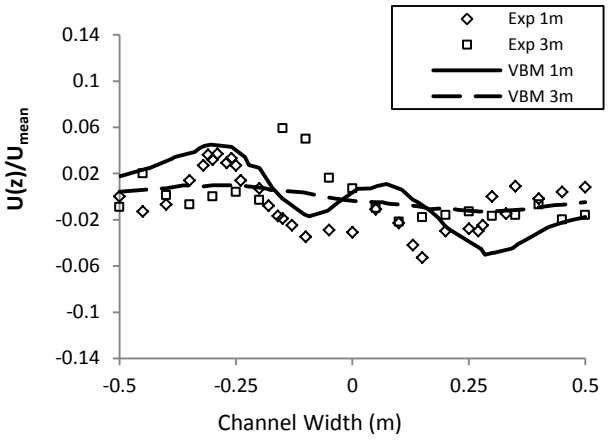

Fig 7. Comparison between experimental and computed lateral velocities across the channel at 1 and 3 meters downstream.

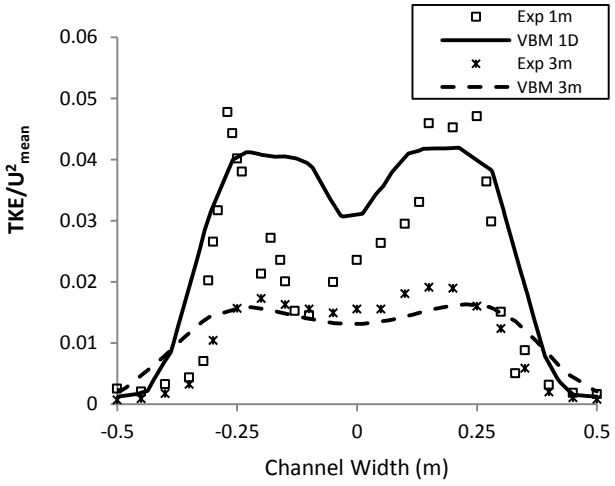

Fig 8. Comparison between experimental data and computed TKE results across the channel at 1 and 3m downstream.

The model was also compared with the experimental measurements of TKE profiles in Fig 8. The overall agreements are fairly good. However there was a slightly underestimation directly behind the HATT (1m) at the tip of the blade and overestimation at the centre. This is due to the assumption made in the VBM that the rotor tip effect cannot be resolved totally: that 96% of the span of the blade experiences lifting and drag and the remaining 4% will only experience drag. The reason for this is because in a realistic scenario a secondary flow at the tip of the blade will be generated. This secondary flow will violate the assumption of the local lift and drag forces being computed in 2D. Therefore, the generation of the secondary flow will be avoided by neglecting the lift force at the tip. However, further downstream at 3m, the agreements improve noticeably.

In general when HATT are employed and energy is extracted, the velocity of flow is consequently reduced. This behaviour will influence the free surface causing it to slightly rise just before the HATT and then drop directly afterwards. Fig. 8 clearly demonstrates such a distribution in the computed results. This is due to the pressure jump caused by the HATT blockage effect. The flow is forced to accelerate around the sides and reducing at the centre forming a surface drop. This behaviour is consistent with previous laboratory scale (Sun et al. 2008) and computational (Bryden et al. 2004) investigations.

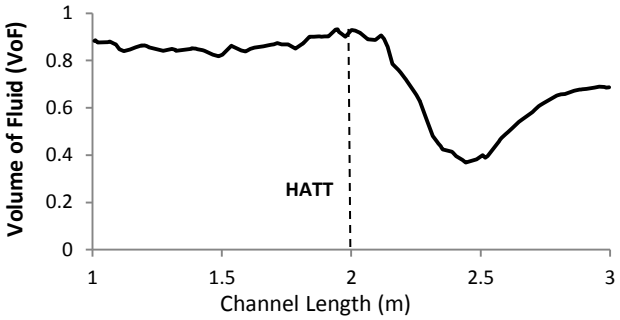

Fig 8. Distribution of computed free surface elevation across the length of the channel.

CONCLUSION

A 3D CFD model based on FLUENT 14.5 was developed to simulate the wake characteristics behind a HATT by solving the RANS equations. The HATT was presented by a VBM approach which solves the BEMT equations. Comparing with the detailed laboratory data, the model has successfully modelled the flow behaviour behind the HATT in the near and far regions in both velocities and turbulent characteristics. The multiphase model was also able trace the free surface behaviour by illustrating a surface rise followed by a sudden drop which was consistent with previous investigations. The model is able to be upgraded to include waves and to be applied for different angles of attack.

ACKNOWLEDGEMENT

The current study is partially supported by the University of Liverpool. Dr Pool and Miss Tedd's assistance in laboratory data supply is also much appreciated.

REFERENCES

ANSYS, I. 2010. ANSYS Fluent Theory Guide, 13 pp.

Barnsley, M.J., and J.F. Wellicome. 1993. Dynamic models of wind turbines—aerodynamic model development. Final Report on contract JOUR 0110 for the Commission of the European Communities Directorate-General XII Science, *Research and Development.*

Bryden, I.G., T. Grinsted, and G.T. Melville. 2004. Assessing the potential of a simple tidal channel to deliver useful energy, *Applied Ocean Research,* vol. 26, no. 5, 198-204 pp.

Consul, C.A., R.H.J. Willden and S.C. McIntosh. 2011. An investigation of the influence of free surface effects on the hydrodynamic performance of marine cross-flow turbines, *Proceeding of Euro Wave Tidal Energy Conference*.

Douglas, C.A., G.P. Harrison, and J.P. Chick. 2008. Life cycle assessment of the Seagen marine current turbine, *Proceedings of the Institution of Mechanical Engineers, Part M: Journal of Engineering for the Maritime Environment,* vol. 222, no. 1, 1-12 pp.

Drela, M., M. Aero, and A.H. Youngren. 2001. XFOIL 6.9 User Primer, *Aerocraft, Inc*.

Malki, R., A.J. Williams, T.N. Croft, M. Togneri, and I. Masters. 2013. A coupled blade element momentum – Computational fluid dynamics model for evaluating tidal stream turbine performance, *Applied Mathematical Modelling,* vol. 37, no. 5, 3006-3020 pp.

Menter, F.R. 1993. Zonal Two Equation k-ω Turbulence Models for Aerodynamic Flows, *Turbulence, Heat and Mass Transfer 4, Germany,* 1993-2906 pp.

Michael, R. 2005. Unstructured, Multiplex Rotor Source Model With Thrust And Moment Trimming - Fluent's VBM Model, *FLUENT*.

Mozafari, A.T.J. 2010. *Numerical modeling of tidal turbines: Methodology Development and Potential Physical Environmental Effects*, University of Washington.

Sun, X., J.P. Chick, and I.G. Bryden. 2008. Laboratory-scale simulation of energy extraction from tidal currents, *Renewable Energy,* vol. 33, no. 6, 1267-1274 pp.

Tedds, S.C., R.J. Poole, and I. Owen. 2012. Experimental investigation of horizontal axis tidal stream turbine, *Ocean Energy*.

Williams, A.J., T.N. Croft, I. Masters, M.R. Willis, and M. Cross. 2010. Combined BEM-CFD modelling of tidal stream turbines using site data, *Proceedings of the International Conference on Renewable Energies and Power Quality*.